ELSEVIER

Ceramics International 30 (2004) 1513–1516

CERAMICS INTERNATIONAL

www.elsevier.com/locate/ceramint

Reactive ion etching of sol–gel-derived BST thin film

Peng Shi*, Xi Yao, Liangying Zhang

Electronic Materials Research Laboratory, Key Laboratory of the Ministry of Education, Xi'an Jiaotong University, Xi'an 710049, China

Received 28 November 2003; received in revised form 10 December 2003; accepted 22 December 2003

Available online 25 June 2004

Abstract

Perovskite (Ba,Sr)TiO_3 (BST) thin film is promising dielectric and ferroelectric material for future generation integrated DRAMs, MEMS, and other devices. The etching properties of BST films were widely concerned. The etching characteristics of sol–gel-derived BST films were investigated in a reactive ion etching (RIE) setup using CHF_3/Ar plasma. The morphology and etching rate were measured by atomic force microscopy (AFM). The surface states of each element in BST films were examined by X-ray photoelectron spectroscopy (XPS). The etching mechanism of BST thin film in RIE was the cooperation of ion bombardment, ions assist chemical reaction and reaction etching effects. The highest etching rate of BST films was 5.1 nm/min.

Keywords: BST; Thin Film; RIE; Sol–gel; CHF_3

1. Introduction

Perovskite (Ba,Sr)TiO_3 (BST) thin film was promising dielectric and ferroelectric material with the properties of high dielectric constant, low leakage current density, and low dielectric loss. These properties gave a possibility to suitable for future generation integrated dynamic random access memories (DRAMs) [1], nonvolatile ferroelectric random access memories (NVFRAM) [2], and microelectromechanical systems (MEMS) [3].

In order to realize highly integrated devices involving BST thin films, it was crucial to develop etching processes providing simultaneously near vertical sidewall angle, fence-free profile, good selectivity over resist, no sidewall residues, and high etch rates. In this context, several studies of the etching properties of the BST thin films had been conducted using high-density plasmas, such as electron cyclotron resonance (ECR), helicon, or inductively coupled plasmas (ICP) in various gas mixtures [4]. However, it was not clear whether or not these processes were really optimum. The etching mechanism of BST films was still not clear.

Moreover, BST thin films were relatively new material involved in microelectronics technology. Therefore, the majority of work was focused on technological aspects, while the etching mechanisms had yet to be focused. Fabrication of BST thin films had been reported by different techniques such as radio frequency (RF) magnetron sputtering [5], liquid source misted chemical deposition [6], metal organic chemical vapor deposition [7], metal organic decomposition [8], and sol–gel process [9]. The sol–gel technique had been widely accepted in the processing of thin films because of its many advantages such as, easier composition control, better homogeneity, low processing temperature, fabrication of large area thin films, and low equipment cost.

In this paper, BST thin films were prepared on SiO_2/Si(1 0 0) substrate by a modified sol–gel method. The films were etched using CHF_3/Ar plasma in a reactive ion etching setup.

2. Experiment

The precursor solution was prepared by acetic acid based sol–gel route. Barium acetate ($Ba(CH_3COO)_2$), strontium acetate ($Sr(CH_3COO)_2 \cdot 1/2H_2O$), and tetrabutyl titanate ($Ti(CH_3CH_2CH_2CH_2O)_4$) were used as starting materials. Glacial acetic acid (CH_3COOH) was used as solvent. Lactic acid ($CH_3CH(OH)COOH$) was used as stabilizer agent. The composition of precursor was $(Ba_{0.70}Sr_{0.30})TiO_3$ and the concentration was 0.4 mol/l.

The precursor solution was spun onto the silicon substrate at 3500 rpm for 30 s. The wet film was baked at 400 °C for

* Corresponding author. Fax: +86-29-82668794.
E-mail address: spxjy@mailst.xjtu.edu.cn (P. Shi).

0272-8842/$30.00 © 2004 Elsevier Ltd and Techna Group S.r.l. All rights reserved.
doi:10.1016/j.ceramint.2003.12.125

20 min before next deposition. Four deposition cycles were repeated to prepare thick film. The films were annealed at 800 °C for 1 h to form the perovskite phase.

BST films were etched in a reactive ion etching setup using CHF_3/Ar plasma. The etching samples were patterned using a conventional photoresists with the standard lithographic process. The effects of the concentration of the etching gases and the RF power were researched.

The surface states of each element in BST film were examined by X-ray photoelectron spectroscopy (XPS). The etching rate and morphology of the films were investigated by atomic force microscopy (AFM).

3. Results and discussions

3.1. Etching rate

Fig. 1 shows the effects of RF power on the etching rate of BST thin film as a function of Ar/(Ar + CHF_3) gas-mixing ratio. The etching rate increased with the increase of RF power when the gas flow rate was 30 sccm. Moreover, the etching rate could be improved by adding Ar gas in plasma. Collision of the reactive ions in the plasma could promote the chemical reactions on the surface of the film.

Christophorous et al. [10] had reported that neutral particles were produced by the attachment of electron and molecules in the range of relative low RF power. With the RF power increasing, the density of active ions and radicals increased simultaneously. The more reactive radicals were produced to improve the etching effects. Moreover, the electron impact and particle collision increased with the increase of RF power. The etching rate increased as more ions drawn onto the film surface. These effects could be explained by the increasing efficiency of both physical and chemical etching. The etching process of BST films was the combination of both physical and chemical effects, including bombardment, attaching on and removing off the surface layer. The role of ion bombardment included physical sputtering of main material, destruction of oxide bonds to promote chemical reactions between Ba, Sr, and Ti with fluorine atoms, and removing the low volatile Ba and Sr fluorides from the surface. Chemical mechanism supported the interaction of F radicals with metals in the surface buffer layer.

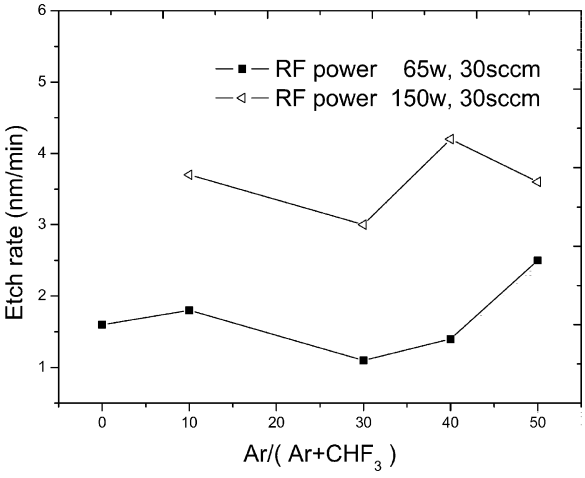

Fig. 1. The etch of BST thin film as a function of Ar/(Ar + CHF_3) gas-mixing ratio with the total flow rate as 30 sccm.

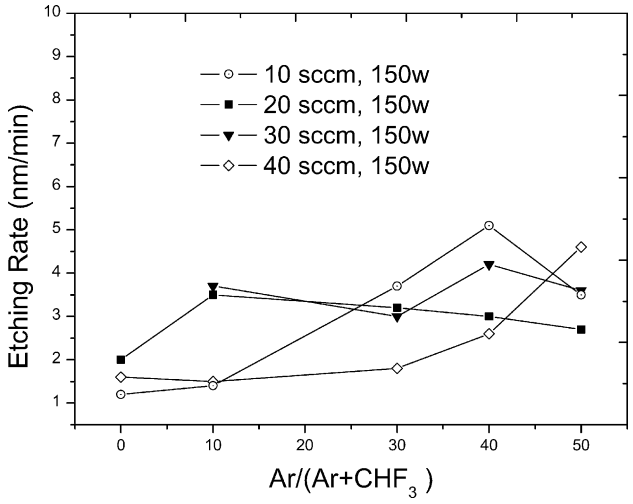

Fig. 2. The etch of BST thin film as a function of Ar/(Ar + CHF_3) gas-mixing ratio with the RF power as 150 W.

Fig. 2 indicated that etching rate did not increase linearly and continually with the increase of the flow rate of etching gases. The collision of particles increased with increasing of the flow rate of mixing gases. When excess etching gas introduced, a thin passivation layer was formed on the film surface, which lead to low etching rate. Furthermore, gas pressure increasing usually caused the decrease of ion bombardment due to the decrease of ion mean free path and energy. Therefore, it was not effective to increase the etching rate by increasing the gas flow rate only.

As the low volatility of reaction products such as Ba and Sr fluorides, the etching of BST thin film were dominated by ion bombardment and ion assist reaction, while the contribution of chemical mechanism could be negligible.

3.2. XPS analysis

The surface states of each element in BST films before and after etching were examined by XPS. The XPS data were shown in the Fig. 3 by comparing the four narrow-scan spectra of Ba_{3d}, Sr_{3d}, Ti_{2p}, and O_{1s}, respectively.

Fig. 3a shows Ba_{3d} narrow-scan spectra of BST films before and after etching. The main peaks at 783.1 and 798.5 eV were identified as a signal of binding energies from Ba–O bonds. Nevertheless, the spectra showed a small shift to higher energy region in comparison with as-deposited film. This shift confirms the chemical reaction between Ba and F [11].

Fig. 3b was the narrow spectra of Sr_{3d} before and after etching. There was a wide maximum in the spectra of

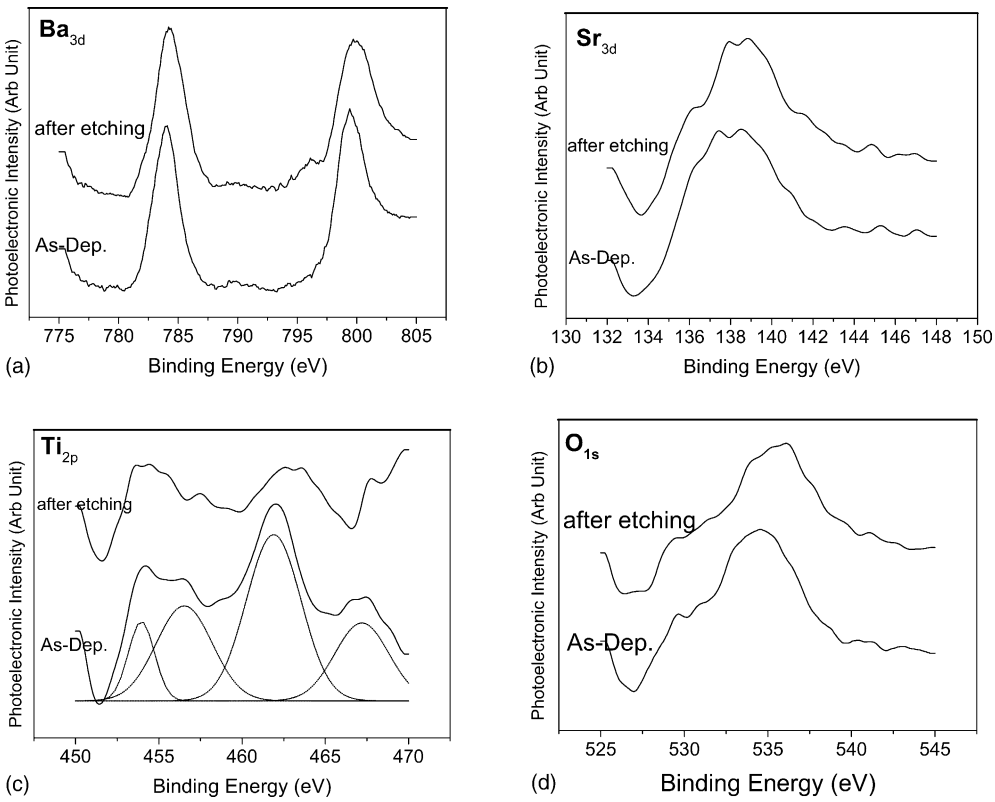

Fig. 3. (a) Ba_{3d}, (b) Sr_{3d}, (c) Ti_{2p}, (d) O_{1s} XPS narrow-scan spectra of BST surface etched under CHF_3/Ar (total flow rate: 30 sccm, $Ar/(Ar + CHF_3)$ ratio: 0.3, RF power: 150 W).

as-deposited film, which might be resolved in two peaks of $Sr_{3d_{5/2}}$ and $Sr_{3d_{3/2}}$ at 137.3 and 138 eV. They were identified as the binding energy of Sr–O. Sr–F peak with binding energy 136 eV appeared in spectra of BST film after etching. This fact confirmed the chemical etching of BST thin films.

In Fig. 3c, spectra of as-deposited film consisted of four peaks. The spectra curve was fitted by Gaussain multi-peaks fit method. The two peaks of $Ti_{2p_{3/2}}$ and $Ti_{2p_{1/2}}$ with energies 461.4 and 467 eV related to TiO_2. The peaks of $Ti_{2p_{3/2}}$ and $Ti_{2p_{1/2}}$ at 454 and 456 eV binding energy related to TiO. All peaks belonged to Ti–O bond. After etching, the intensity of Ti–O peaks sufficiently decreased, while no new peaks appeared. It meant that Ti–O bonds were destroyed by chemical reaction as well as ion bombardment. The ion bombardment played a dominant role in etching mechanism.

3.3. AFM images

Fig. 4 shows the AFM images of BST film before and after etching. The surface structure of as-deposited film was compact and the grain size of aggregation was about 200 nm in diameter with the height about 20 nm. The roughness of

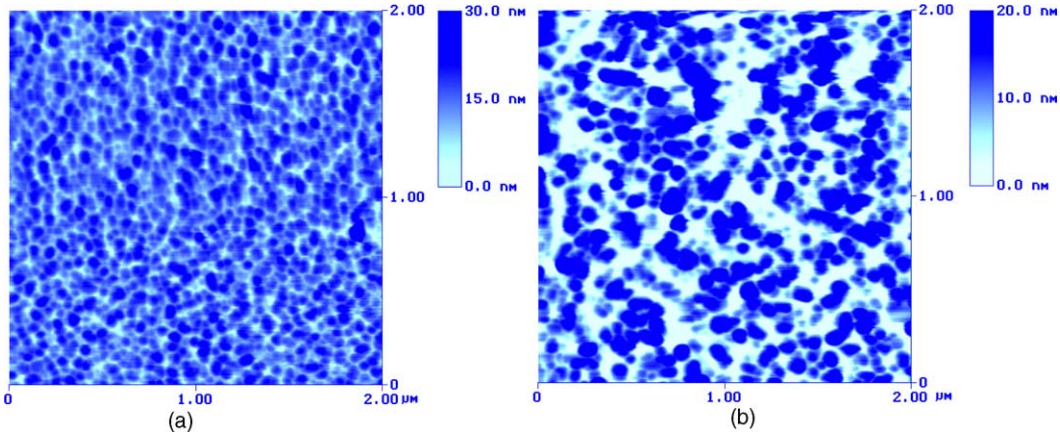

Fig. 4. AFM image of BST: (a) before etching, (b) after etching (total flow rate: 30 sccm, $Ar/(Ar + CHF_3)$ ratio: 0.3, RF power: 150 W).

surface film was characterized by the r_{ms} (r_{ms} was defined as the root mean square). Etched films at CHF_3/Ar RIE for 10 min had a r_{ms} of 7.656 nm in comparison with a r_{ms} around 3.922 nm for unetched films. The depth of pits and holes around the grain was deeper than that before etching. The compactness of surface layer after etching in plasma was deteriorated. From the figures, it can be seen that the joining section between grains was easy to etch by ion bombardment or/and ion assist chemical reaction. There was a preference etch at the grain boundaries in the film.

4. Conclusions

The etching mechanism of BST thin film in RIE system was the combination of ion bombardment, ions assist chemical reaction and reaction etching effects. The etching rate increased with the increase of RF power and vacuum pressure. The gas flux was not dominant to the increasing of etching rate. In our work, the etching rate could reach to 5.1 nm/min when the power was 150 W, the total gas flow rate was 10 sccm and the ratio of CHF_3 to Ar was 3/2. The etching rate was relative low because of the lower density of active ions and the low volatility of reaction products.

Acknowledgements

This work was supported by the Ministry of Sciences and Technology of China through 973-project under Grant 2002CB613305 and the International Joint Research Project of China–Israel (time: 2002–2003).

References

[1] G.A. Hirata, L.L. López, J.M. Siqueiros, J. McKittrick, Ferroelectric $Ba_{1-x}Sr_xTiO_3$ thin films for DRAM's applications, Superficies Vacio 9 (1999) 147–149.
[2] S. DeOrnellas, P. Rajora, A. Cofer, Challenges for plasma etch integration of ferroelectric capacitors in FeRAM's and DRAM's, Integr. Ferroelectrics 17 (1–4) (1997) 395–402.
[3] M. Azuma, M.C. Scott, C.A. Par De Araujo, J.D. Cuchiaro, US Patent 08 165 082, 27 December, 1999.
[4] D.S. Wuu, C.C. Lin, R.H. Horng, F.C. Liao, Y. H, Etching characteristics and plasma-induced damage of high-k $Ba_{0.5}Sr_{0.5}TiO_3$ thin-film capacitors, J. Vac. Sci. Technol. B (Microelectron. Nanometer Struct.) 19 (6) (2001) 2231–2236.
[5] J.C. Shin, J.H. Park, C.S. Hwang, H.J. Kim, Dielectric and electrical properties of sputter grown (Ba,Sr)TiO_3 thin films, J. Appl. Phys. 86 (1) (1999) 506–513.
[6] H.J. Chung, J.H. Choi, J.Y. Lee, S.I. Woo, Preparation and electrical properties of (Ba,Sr)TiO_3 thin films deposited by liquid source misted chemical deposition, Thin Solid Films 382 (2001) 106–112.
[7] C.Y. Yoo, H.B. Park, D.S. Hwang, H. Hideki, W.D. Kim, H.J. Lim, B.T. Lee, Y.W. Park, S. Lee, M.Y. Lee, Integration issues of (Ba,Sr)TiO_3 thin films in high density devices, Ferroelectric Thin Films VIII (2000) 11–23.
[8] S.B. Krupanidhi, C.J. Peng, Studies on structural and electrical properties of barium strontium titanate thin films developed by metallo-organic decomposition, Thin Solid Films 305 (1/2) (1997) 144–156.
[9] N.V. Giridharan, R. Varatharajan, R. Jayavel, P. Ramasamy, Fabrication and characterisation of (Ba,Sr)TiO_3 thin films by sol–gel technique through organic precursor route, Mater. Chem. Phys. 65 (2000) 261–265.
[10] L.G. Christophorous, J.K. Olthoff, M.V.V.S. Rao, Electron interactions with CHF_3, J. Phys. Chem. Ref. Data 26 (1) (1997) 1–15.
[11] P.S. Kang, K.T. Kim, D.P. Kim, C.I. Kim, A.M. Efremov, Dry etching characteristics of (Ba,Sr)TiO_3 thin films in high density CF_4/Ar plasma, Surf. Coat. Technol. 171 (2003) 273–297.